

INPE-5578-PRE/ 1806

**ON THE OPTIMIZATION OF SPECKLE FILTERING TECHNIQUES FOR
ERS-1 IMAGES OVER ARGENTINA**

Alejandro Cortese
Laura Frulla
Julio Jacobo-Berlles
Marta Mejail
Alejandro C. Frery

Paper present at the International Symposium on Resource and
Environment Monitoring, Rio de Janeiro, 26-30 Sept. 1994

INPE
São José dos Campos
1994

On the Optimization of Speckle Filtering Techniques for ERS-1 Images over Argentina

Alejandro Cortese¹ Laura Frulla² Julio Jacobo-Berlles¹ Marta Mejail¹ Alejandro C. Frery³

¹Computer Science Department
University of Buenos Aires
Pabellón I
Ciudad Universitaria
1428 Buenos Aires
Argentina

²CAERCEM
Julián Álvarez 1218
1414 Buenos Aires
Argentina

³INPE – Instituto Nacional de Pesquisas Espaciais
DPI – Divisão de Processamento de Imagens
Avenida dos Astronautas, 1758
12227-010 São José dos Campos
SP – Brazil

Keywords: filters, robustness, SAR image processing, speckle noise reduction.

ABSTRACT

SAR images provide detailed information about the target surface, though it is obscured by the well-known speckle effect. One alternative of speckle reduction is by filtering the image, but this demands some assumptions about the speckle behaviour. However, it is important to take into account that noise reduction filters tend to blur the edges and sharp features of the images, since they always introduce some kind of low pass effect. Several filters have been developed for the speckle reduction, and most of them are of the form of a window that slides over the image. But there is no automatic process to determine the window size, a relevant parameter that depends, among other things, on the features of the studied area. Given a filter, it can be applied to the SAR image for different window sizes; then it is possible to estimate the so-called speckle index as a measure that provides the best speckle reduction in accordance to the degree of heterogeneity of the region under study. In this paper the type of filter which better reduces the speckle in homogeneous and heterogeneous regions is determined. Moreover, it is possible to draw conclusions about the optimal window size used when the filter is applied.

1. INTRODUCTION

The gray level of each pixel in a one-look SAR image acquired using a linear detector is (under certain conditions) a random variable Y with a Rayleigh distribution ($Y \sim \mathcal{R}(\xi)$) where ξ is the backscatter coefficient, so

$$f_{\xi}(y) = \frac{y}{\xi^2} \exp\left[-\frac{1}{2}\left(\frac{y}{\xi}\right)^2\right],$$

for $y > 0$. This coefficient depends on the electromagnetic properties of the surface at the considered frequency, polarization and incidence angle of the electromagnetic radiation emitted by the SAR antenna. For a Rayleigh distributed random variable, its mean and variance are related by

$$\sigma_Y = \left(2\sqrt{\frac{1}{\pi} - \frac{1}{4}}\right)\mu_Y,$$

thus the standard deviation is roughly one half the mean value. Then, given a homogeneous area, with uniform backscatter coefficient, its appearance will be very noisy. This phenomenon is called *speckle*.

One way of reducing the speckle is to increase the number of looks, other way is to filter the image.

In this paper various filters with robust properties are applied to synthetic SAR images, their performances are analyzed and the effect of the window size is evaluated.

2. SPECKLE NOISE FILTERS

Several techniques for filtering whilst preserving relevant features in images have appeared in the literature (see [Nagao-Matsuyama (1979)], for example).

Some specialized filters have been proposed aiming at the reduction of speckle noise and, simultaneously, not blurring the image. The reader is referred to the papers [Frost et al. (1982)], [Lee (1981a, 1981b)], [Nathan-Kurlander (1987)], and to the references therein for details. Some of them are summarized in the following list:

- Mean filter: it consists of a local smoothing of the observations. It also normalizes the filtered image, but introduces severe blurring.
- Frost filter: it is a linear convolutional proposal, derived from the minimization of the mean quadratic error over a multiplicative noise model. Dependence among observations is incorporated through an exponential spatial correlation function. It is adaptive.
- σ -Lee Filter: it assumes a normal distribution, and trims those observations beyond the $2\hat{\sigma}$ interval.
- Lee Filter: a multiplicative noise model is adopted. It is a local linear minimum mean square error filter, since it uses a linearization, by Taylor expansion, around the mean. This approximation transforms the multiplicative model into an additive one, and then the Wiener filter is applied.
- Kuan/Nathan Filter: it is similar to the previous one. The difference is that this filter does not

make any approximation. It is, also, an adaptive proposal.

3. ROBUST FILTERS

In this work two kinds of robust estimators will be considered: two based upon the idea of *trimming* extremal observations, and three based on *order statistics* [Frery-Sant'Anna (1993a, 1993b)].

Proceeding with the idea that *filtering* is *estimating*, and taking into account the possibility of having a contaminated sample of observations, the use of the following estimators is proposed (they are all based upon the sample y_W , of size v , where y is the vector of observations (y_1, \dots, y_v)):

$$\begin{aligned}\xi_{\text{TML}} &= \sqrt{\frac{1}{2(v-2a)} \sum_{i=a+1}^{v-a} y_{v,i}^2} \\ \xi_{\text{TMO}} &= \sqrt{\frac{2}{\pi} \frac{1}{v-2a} \sum_{i=a+1}^{v-a} y_{v,i}} \\ \xi_{\text{MAD}} &= \frac{1}{K_1} Q_2(z) \\ \xi_{\text{IQR}} &= \frac{Q_3(y) - Q_1(y)}{K_2} \\ \xi_{\text{MED}} &= \frac{1}{K_3} Q_2(y)\end{aligned}$$

where $a = \lfloor v\alpha_0 \rfloor$, $0 \leq \alpha_0 < 1/2$, and $(y_{v,1}, \dots, y_{v,v})$ denotes the vector y sorted in ascending order; $z = (z_1, \dots, z_v)$, with $z_i = |y_i - Q_2(y)|$ for every $i \in W$. $Q_1(y)$, $Q_2(y)$ and $Q_3(y)$ denote the lower sample quartile, the sample median and the upper sample quartile of y , respectively. The trimmed observations are the $\lfloor v\alpha_0 \rfloor$ smallest and the $\lfloor v\alpha_0 \rfloor$ biggest ones.

The estimators above are, respectively, the *trimmed ML* estimator with a proportion of deleted observations equal to $2\alpha_0$, the *trimmed MO* estimator with a proportion of deleted observations equal to $2\alpha_0$, the MAD (Median of the Absolute Median Deviation) estimator, the IQR estimator based on the inter-quartile range, and the Median estimator.

The constants K_1 , K_2 , K_3 are calculated in order to make the respective estimators asymptotically consistent.

4. ADAPTIVE WINDOW

In [Changle Li (1988)] the variance ratio R is defined as

$$R = \frac{\sigma_x^2}{\sigma_y^2}$$

where x is the true image, y is the observed image, and they are related by $y = xn$, being n the noise. For this model, it can be proved that

$$R = \frac{1 - \left(\frac{\mu_n \sigma_n}{\sigma_y}\right)^2}{1 + \sigma_n^2}$$

so $R \in [0, 1]$. Values close to 0 indicate that the region considered is smooth, and values close to 1 indicate a zone with fine detail. In [Mascarenhas et al. (1991)] a correspondence between R and a certain window size is established, dividing the range between 0 and 1 in five subranges and assigning them window sizes from 9×9 to 1×1 ; R is then used to adaptively determine the window size to process each pixel of the image.

5. RESULTS

The used filters were: ML, MO, TML, TMO, MAD, IQR and MED. They were applied to synthetic images, generated with the Rayleigh distribution. Two different versions of each filter were utilized: fixed window size and adaptive window size. The fixed window sizes were 3×3 , 5×5 , 7×7 and 9×9 , whilst the adaptive window size was determined using R which was calculated on windows of size 7×7 for each pixel.

For each original image, an image I_R was generated from the values of the coefficient R , calculated for each pixel over a window of size 7×7 . Then, this images were used to apply the adaptive versions of the filters utilizing the corresponding of values of I_R to determine window sizes. So, in each filtered image, each pixel y'_{ij} was generated using a window size that depends on $I_{R_{ij}}$.

The synthetic images have two regions, with values of backscatter ξ_1 (B1) and ξ_2 (B2), given in the following table.

B1	20	30	40	50	60
B2	120	110	100	90	80

The third case, namely $\xi_1 = 40$ and $\xi_2 = 100$ was taken as the one that best reflects real data.

The coefficients of skewness and kurtosis of the random variable X (denoted γ_1 and γ_2), if they exist, are given, respectively, by:

$$\gamma_1 = \frac{E(X - E(X))^3}{(\text{Var}(X))^{3/2}},$$

$$\gamma_2 = \frac{E(X - E(X))^4}{(\text{Var}(X))^2} - 3,$$

where $\text{Var}(X) = E(X^2 - (E(X))^2)$ is the variance of X . These values relate the symmetry and heavy-tailedness (how quickly the tails of the density fall off to zero) of its distribution [Lewis-Orav (1986)]. For normally distributed random variables, these quantities are identically zero.

The results, for the third case, are presented in the following tables.

	C	S	K
Original	1.92	0.64	0.36

3x3 Window

ML	5.96	0.18	0.17
MO	5.76	0.21	0.06
TML	5.18	0.22	-0.06
TMO	5.01	0.25	-0.04
MAD	2.42	0.59	0.32
IQR	3.06	0.42	0.02
MED	4.37	0.26	0.10

5x5 Window

ML	9.86	0.08	0.09
MO	9.59	0.08	-0.02
TML	8.34	0.09	-0.08
TMO	8.19	0.10	-0.07
MAD	4.14	0.36	0.24
IQR	4.60	0.28	0.15
MED	7.11	0.21	0.09

7x7 Window

ML	13.57	0.04	0.03
MO	13.12	0.06	-0.11
TML	11.42	0.04	-0.18
TMO	11.27	0.04	-0.15
MAD	5.94	0.16	0.22
IQR	6.21	0.14	0.06
MED	9.94	0.13	0.12

9x9 Window

ML	17.55	0.02	-0.11
MO	17.06	0.09	-0.22
TML	14.50	0.09	-0.13
TMO	14.26	0.09	-0.13
MAD	7.52	-0.09	0.18
IQR	7.78	0.01	0.08
MED	12.93	0.08	0.08

R Window

ML	16.97	-0.02	0.06
MO	16.31	-0.05	0.09
TML	13.69	-0.14	0.36
TMO	13.45	-0.17	0.41
MAD	7.20	0.12	0.42
IQR	7.45	0.14	0.35
MED	12.21	-0.17	0.61

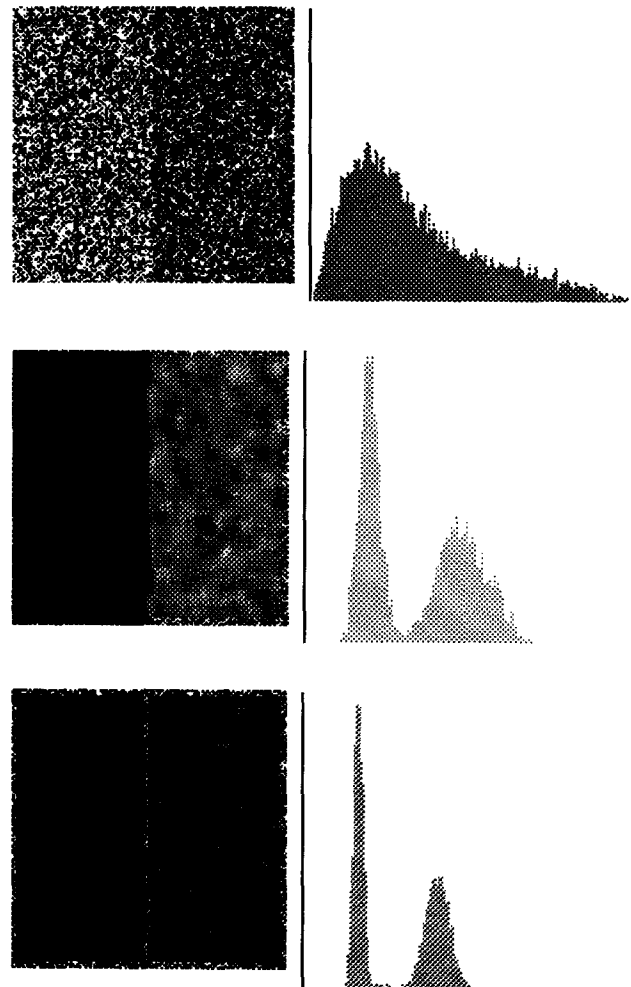
From these tables, it can be concluded that the adaptive (R) window produces similar results to the 9×9 one. The advantage of using the latter is that it is of fixed size, requiring no adaptive technique; while the use of the former may preserve better borders and sharp features. Since the considered images consist mostly of homogeneous areas, it is sensible that large windows appear.

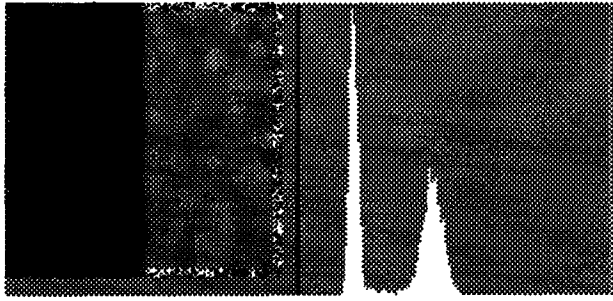
The performance of the considered filters was assessed using the following sample quantities: the reciprocal of the coefficient of variation (C), the skewness (S) and the kurtosis (K). The following table shows which filter, for the condition

$\xi_1 = 40$ and $\xi_2 = 100$, was the best for each of the aforementioned criteria, i.e., the table shows which filter attains $\max\{\hat{C}\}$, $\min\{|y_1|\}$ and $\min\{|y_2|\}$.

	C	S	K
3x3	ML	ML	IQR
5x5	ML	MO	MO
7x7	ML	TMO	ML
9x9	ML	IQR	IQR
R	ML	ML	ML

For the sake of visual comparison, the original and some filtered (IQR and TMO with window size 7×7 , and TML with R size window) images are shown with their respective histograms in the following figures. Notice that the pixels located close to the borders of the image remain unfiltered.





6. CONCLUSIONS

From the point of view of noise reduction of the resulting image, the criterion given by the inverse of the sample coefficient of variation $(\hat{C})^{-1}$ indicates that the best performance is obtained with the ML filter. If the criterion is the normality of the filtered data (measured by its skewness and kurtosis), there are various filters that perform equally well.

The results obtained with the adaptive window are consistent with the used data.

The quantitative assessment of detail preservation properties of filters is not straightforward. Some contributions have been made in this direction, for speckle filters, in [Sant'Anna, 1994] with the use of spectral techniques and border detectors.

These filters will be applied to 1-look ERS-1 SAR images over Argentina. It is expected that the filters will reduce the overall noise, while preserving details and sharp features.

7. REFERENCES

- Changle Li. Two Adaptive filters for speckle reduction in SAR images by using the variance ratio. *International Journal of Remote Sensing*, 9(4):641-653, 1988.
- Frery, A.C.; Sant'Anna, S.J.S. Redução de ruído em imagens SAR pelo uso de filtros robustos. In: Simpósio Brasileiro de Sensoriamento Remoto, 7., Curitiba, 10-14 maio 1993. *Anais*. São José dos Campos, INPE, 1993a, v. 3, p. 433-443.
- Frery, A.C.; Sant'Anna, S.J.S. Non-adaptive robust filters for speckle noise reduction. In: Simpósio Brasileiro de Computação Gráfica e Processamento de Imagens, 6., Recife, PE, Brazil, 19-22 out. 1993. *Anais*. Recife, PE, Brazil, SBC/UFPe, 1993b, p. 165-174.
- Frost, V.S.; Stiles, J.A.; Shanmugan, K.S.; Holtzman, J.C. A model for radar images and its applications to adaptive digital filtering of multiplicative noise. *IEEE Trans. on Pattern Analysis and Machine Intelligence*, PAMI-4:157-166, 1982.
- Kuan, D.T.; Sawchuk, A.A.; Strand, T.C.; Chavel, P. Adaptive restoration of images with speckle. [Washington], SPIE, 1982. p. 28-38. (SPIE Proceeding v. 359).
- Lee, J.S. Speckle analysis and smoothing of synthetic aperture radar images. *Computer Graphics and Image Processing*, 17:24-32, 1981a.
- Lee, J.S. A simple speckle smoothing algorithm for synthetic aperture radar images. *IEEE Trans. on Systems, Man, and Cybernetics*, SMC-13:85-89, 1981b.
- Lewis, P.A.W.; Orav, E.J. *Simulation methodology for statisticians, operations analysts and engineers vol. 1*. Pacific Grove, CA, Wadsworth & Brooks/Cole Advanced Books & Software, 1989, 416 pp.
- Mascarenhas, N.; Ono, S.; Fernandes, D.; Kux, H. A comparative study of speckle reduction filters in SAR images and their application for classification performance improvement. In: 24th International Symposium on Remote Sensing of Environment, Rio de Janeiro, Brazil, 1991.
- Nagao, M.; Matsuyama, T. Edge preserving smoothing. *Computer Graphics and Image Processing*, 9(4):394-407, Apr. 1979.
- Sant'Anna, S.J.S. *Avaliação do desempenho de filtros redutores de "speckle" em imagens de radar de abertura sintética*. (MSc Thesis) - INPE, São José dos Campos, SP, Brazil, to appear in 1994.